Insights on Sewer Geyser Mechanisms and Retrofitting Strategies through Numerical Modeling and Laboratory Measurements

Sumit R. Zanje, Ph.D.¹; and Arturo S. Leon, Ph.D., D.WRE, P.E.²

¹Dept. of Civil and Environmental Engineering, Florida International Univ., Miami, FL.

Email: szanje@fiu.edu

²Dept. of Civil and Environmental Engineering, Florida International Univ., Miami, FL.

Email: arleon@fiu.edu

ABSTRACT

This paper offers a preliminary exploration of sewer geysers, commonly termed sewer blowouts, prevalent in combined sewer systems during intense precipitation. Through extensive large-scale experiments at the Engineering Center of Florida International University and a meticulous 3D numerical modeling approach utilizing OpenFOAM, the study unveils the intricate mechanisms governing geyser formation. The experimental setup, employing a novel approach, provides detailed insights into geyser eruption dynamics, while the numerical model employs a finite volume method, emphasizing a sharp air-water interface. The research introduces and evaluates two retrofitting strategies—Retrofitting Strategy I, involving the enlargement of a dropshaft section, and Retrofitting Strategy II, combining a bypass with an orifice plate. A comparative analysis showcases particular differences in pressure variations and ejection velocities, highlighting the potential of Retrofitting Strategy II in reducing pressure fluctuations. The study concludes that introducing an offset between the lower and upper dropshaft sections enhances the effectiveness of near-surface retrofitting, mitigating visible geyser eruptions. The findings underscore the necessity for ongoing field monitoring to refine and validate these retrofitting strategies. In summary, this paper helps to better understand sewer geysers, amalgamating experimental insights, numerical modeling, and practical retrofitting approaches to address challenges in stormsewer systems, providing a valuable resource for future research and infrastructure planning.

Keywords: 3D numerical modeling, combined sewer system, finite volume method, retrofitting strategies, sewer system.

INTRODUCTION

Sewer geysers, commonly referred to as sewer blowouts, pose a notable predicament that can transpire amidst instances of intense precipitation. These occurrences transpire when the amalgamated sewer system, which transports both wastewater and stormwater, becomes inundated as a result of excessive rainfall, surpassing its threshold for accommodating water volume. Consequently, this situation may engender potential hazards to public well-being, inflict harm upon the integrity of infrastructure, and contribute to the degradation of the surrounding environment. In unraveling the mechanism and attributes of geysers, various hypotheses have been put forth by researchers (Zhou et al., 2002; Vasconcelos and Wright, 2005). The elusive nature of their formation, marked by destructive tendencies, persists due to a scarcity of definitive reports and recorded data. Moreover, there has been a considerable amount of research

dedicated to the computational representation of geysers. Despite the existence of a substantial deficit in our understanding of various aspects related to the occurrence of geysers, up until now, there have been only a limited number of research studies and inquiries (both experimental and numerical) conducted on possible measures for mitigating geysers.

This paper is divided as follows. First, this paper offers a concise overview of recent large-scale experimental endeavors. This provides a comprehensive framework for emulating violent geysers, enabling an in-depth examination of the mechanisms within a laboratory environment that closely resembles those encountered in real-world stormwater and combined sewer systems. Secondly, a succinct overview is provided for a 3D numerical modeling approach aimed at comprehending the geyser phenomenon. Subsequently, two prospective retrofitting strategies are introduced and briefly evaluated for their effectiveness through comparison with a non-retrofitting scenario. Finally, the key findings are summarized.

EXPERIMENTAL WORK

Experimental setup

This research, conducted at the Engineering Center (EC) of Florida International University (FIU) in Miami, FL, focuses on the study of field-scale sewer geysers using the recently developed large-scale hydraulics lab at the EC. The experimental facility, situated outdoors on a 20 ft x 60 ft concrete slab area, is scalable, allowing for the exploration of various flow configurations. State-of-the-art sensors are integrated into the setup to capture rapid variations in pressure, flow, and void fraction data during geyser eruptions. The schematic representation of the experimental setup is depicted in Figure 1, showcasing the comprehensive approach employed in this study. The experimental set-up comprises a flow loop, along with a system for the management and control of fluids, specifically water and air. The flow loop was constructed utilizing interconnected polyvinyl chloride (PVC) sections, measuring 6 inches in diameter and comprising both opaque and clear segments. The connections between these sections were established through 152 mm (6-inch) schedule 80 PVC flanges, forming a loop consisting of horizontal and vertical pipe configurations. The ends of the horizontal pipe were connected to the upstream and downstream metal water tanks. Water flowed from the upstream tank to the downstream tanks through a horizontal pipe loop and circulated back into the upstream tank. The fluid management and control system consists of mechanisms, devices, and components used to ensure the safe storage and control of working fluids. The upstream and downstream tanks are made up of thick metal sheets with two chambers (primary and re-circulation). The total static head of the water in the water tanks can be varied, ranging from 2.5 m to 5 m, by utilizing a sliding gate. In the present study, gravity-driven flow was established by elevating the sliding gates of the upstream and downstream tanks to 4.9 m and 4.85 m, respectively. The water recirculation in the closed loop from the downstream tank to the upstream tank was achieved using a 7.5 HP AMT heavy-duty straight centrifugal pump ($Q_{max} = 440$ GPM, $P_{max} = 150$ psi, $H_{max} = 95$ ft). Compressed air, stored within a horizontal air receiver boasting a capacity of 4 m³ (1060 gallons, 200 psi, 6-inch outlet), was introduced into the horizontal pipe through a high-pressure 6-inch flanged flex connector situated near the upstream water tank.

Experimental procedure

The experimental methodology employed in this study was meticulously designed to establish a dependable and reproducible approach, aimed at acquiring accurate and high-quality

data while mitigating oscillations unrelated to the critical dynamics associated with a violent geyser eruption.

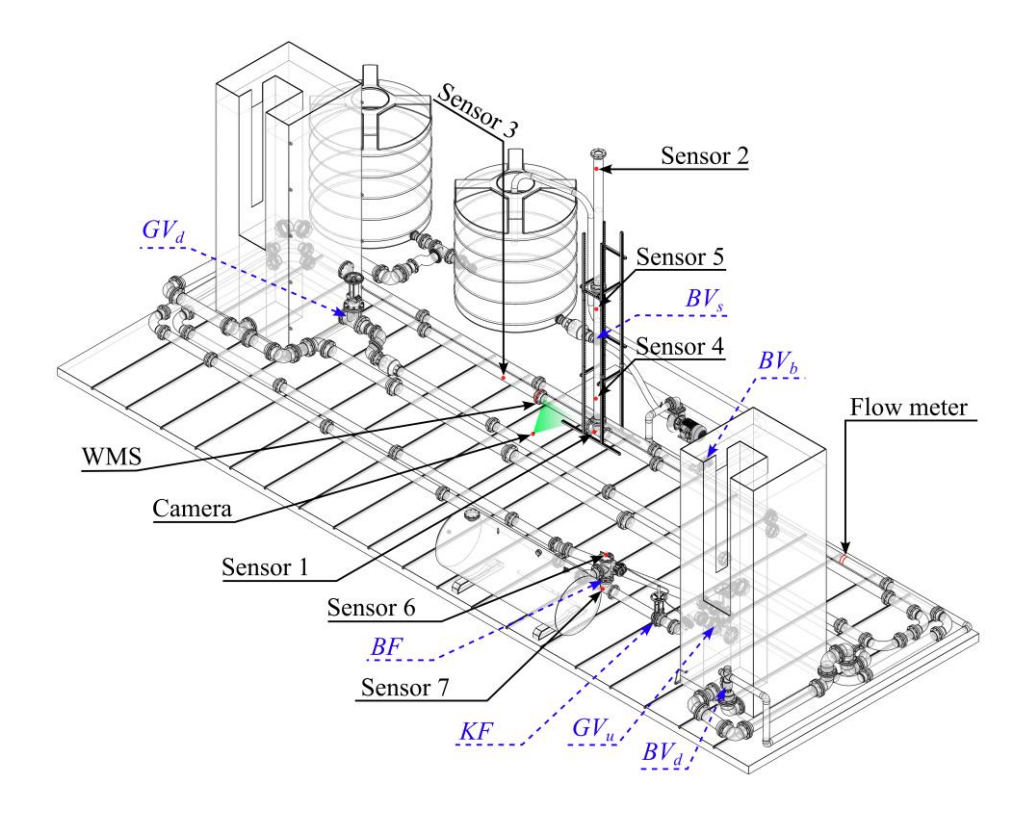


Figure 1: Schematic diagram of experimental facility at the Engineering Center (EC) of the Florida International University, Miami, FL

- 1. Ensure that initially, all the valves (gate valves (GV_u and GV_d), ball valves (BV_s , BV_d and BV_b), butterfly valve (BF), and knife gate valve (KF)) for both the air and water delivery systems are closed.
- 2. Turn on the upstream gate valve (GV_U) , downstream gate valve (GV_D) , knife gate (KF), and ball valves on the suction and discharge lines of the centrifugal pump $(BV_s \text{ and } BV_d)$. Initiate the system filling process until the overflow chambers $(OC_U \text{ and } OC_D)$ of both the metal and plastic tanks are completely filled with water.
- 3. Turn on the centrifugal pump and open the bypass ball valve (BV_b) . Note that shortly, the main chambers $(MC_U \text{ and } MC_D)$ of both the metal tanks will start to overflow, and the water will fall back to the overflow chambers of the respective tanks.
- 4. Once the overflow is observed at the main chambers (MC_U and MC_D) of both the metal tanks, turn on upstream and downstream gate valves (GV_u and GV_d), knife gate valve (KF by 25 %), and the ball valve (BV_b) on the bypass line of the centrifugal pump. Under this setting, 3 to 5 min were allowed to ensure that the flow was fully developed in the flow loop.
- 5. Figure 2 shows an example of a complete time trace of the recorded pressure. Once the system has completed the 'State I', that is, reaches the steady state, the air supply is turned on by opening the butterfly valve (*BF*) slowly at the air receiver tank. Once the *BF* is completely opened, the air advances into the horizontal pipe, causing some disturbance

due to a water spill at the top of the dropshaft. At about 106 s, the disturbances ceased almost completely. Between 106 s to 152 s, the system appears to be in equilibrium, which can be determined by the consistent pressure head readings in the air receiver (sensor 6) and the pressure transducers in the horizontal pipe (sensors 1, 3, and 7). At this point, the pressure heads were equivalent to the water level in the dropshaft. From turning on the *BF* and allowing the system to reach equilibrium, the entire process is marked as 'Stage II' in Figure 2. This stage is important for ensuring that a thin air pocket is formed throughout the horizontal pipe.

- 6. Around the 152-second mark, a gradual and smooth progression of air into the horizontal pipe was observed, and from 187 s to 300 s, eruptions were observed to occur.
- 7. After multiple eruptions, turn off the data recording and save the acquired data with appropriate labeling.

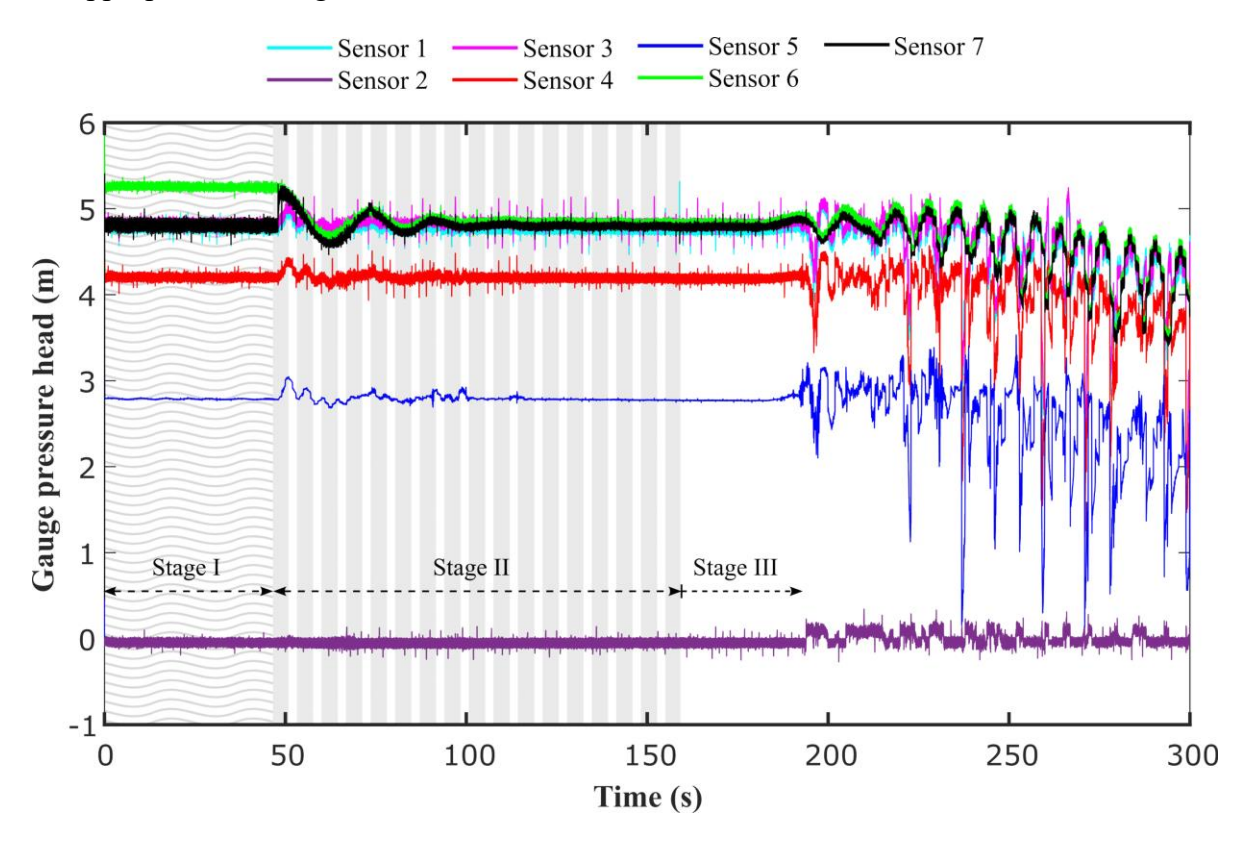


Figure 2. Example of complete time trace of recorded pressure heads

MECHANISMS UNDERLYING THE FORMATION OF GEYSERS

This section briefly outlines the mechanisms observed during experiments that contribute to the formation of geysers. Large air pockets smoothly advance toward the dropshaft without causing significant fluctuations. A significant amount of air enters the dropshaft and ascends in the form of a bullet-shaped bubble, known as the Taylor bubble, which occupies the majority of the pipe cross-section (Leon and Zanje, 2019). The ascending Taylor bubble displaced the water inside the dropshaft, causing spillage at the top of the dropshaft. Note in Figure 3 that pressure fluctuations in the dropshaft (i.e., sensors 1, 4, and 5). Water overflowing from the top of the

dropshaft induces a swift decrease in pressure at the base of the dropshaft, as evidenced by sensor 1 of Figure 3b. This, in turn, triggers a rapid increase in air velocity within the horizontal pipe, resulting in alterations in the flow regime. The rapid depressurization propels the newly formed slugs forcefully into the dropshaft, causing an eruption. Observations suggest that the resulting geyser is not merely a combination of water and air splashing, but rather a violent eruption that closely resembles the documented geysers in various web footages. After a significant eruption (i.e., once the aforementioned liquid slugs traverse the T-junction connecting the horizontal and vertical pipes), a partial blockage occurs, leading to a disruption in the flow. Due to the limited amount of air supplied from the horizontal pipe (as a result of a temporary blockage at the T-junction), the liquid film within the dropshaft slows down and descends towards the T-junction. It is apparent that during this process (i.e., the fluctuation in pressure associated with each rapid eruption), new slugs are formed within the horizontal pipe. The study demonstrates that subsequent eruptions can be observed in the system as long as a continuous supply of water and air is maintained.

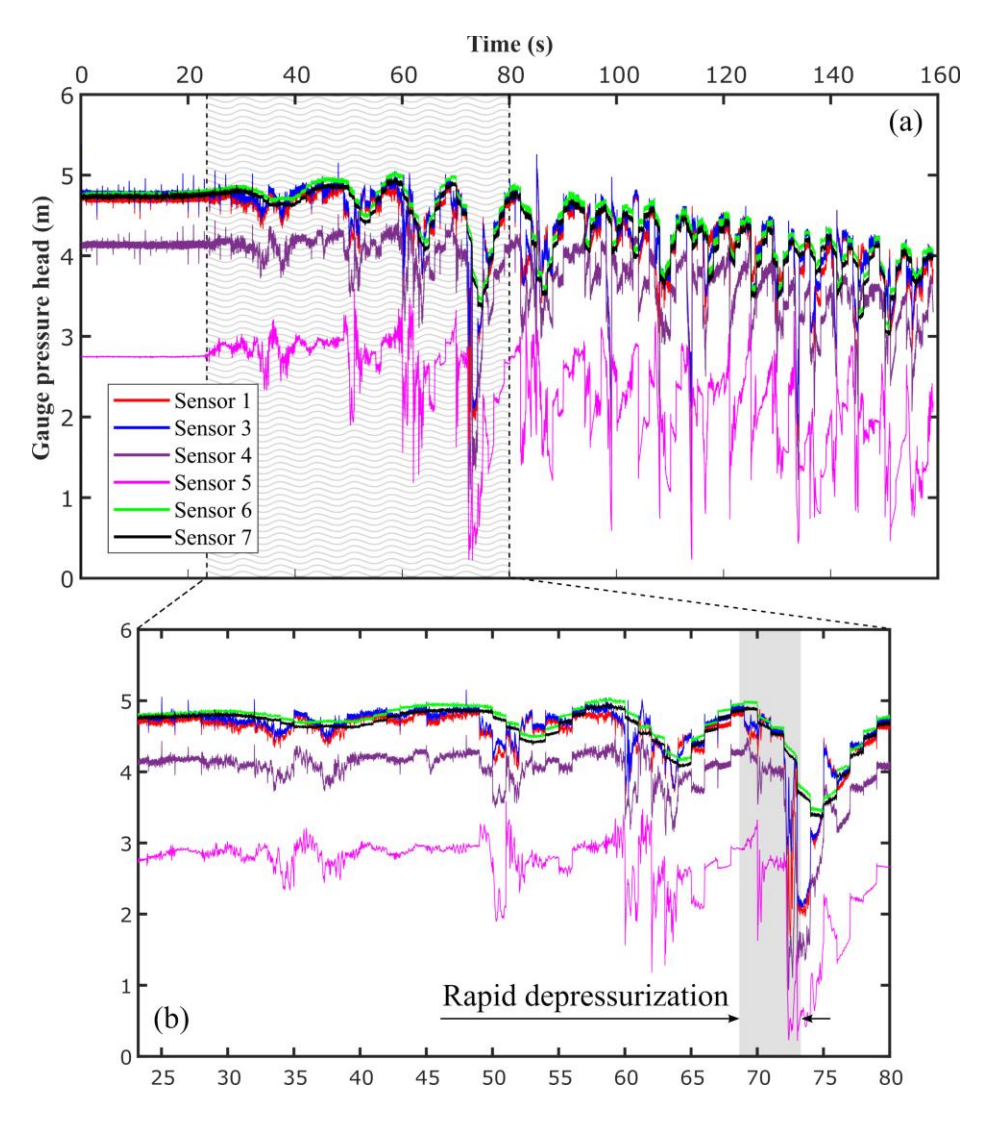


Figure 3. Example of pressure head for explaining the mechanism: (a) time trace in stage III, (b) zoom-in

NUMERICAL MODELING

The numerical methods used in this work rely on a cell-centered, co-located finite volume method (FVM), which is implemented using the open-source CFD software OpenFOAM V6. The present finite volume code is based on the pressure-based two-phase solver compressibleInterFoam. This solver uses the three-dimensional (3D) equations for two phases, i.e., air and water, using the volume of fluid (VOF) method with special emphasis on maintaining a sharp free surface (interface-capturing) (Zanje et al., 2022a,b). This method uses the volume fraction indicator function α to determine the amount of liquid present in each cell. In this study, $\alpha = 1$ and $\alpha = 0$, the cell volume is considered filled with water and air, respectively. A schematic of this numerical set-up is shown in Figure 4. The model comprised of the subsequent components: (1) a complete upstream horizontal pipe $(Lu_1 + Lu_2)$ measuring 40 m in length and 0.152 m in diameter, (2) a horizontal downstream pipe (Ld) measuring 6 m in length and 0.152 m in diameter, (3) a continuous air supply introduced into the upstream horizontal pipe at a location 30 m away from the furthest upstream point, (4) a dropshaft measuring 6.096 m in length with a diameter of 0.152 m, located at a distance of 40 m from the furthest upstream point, and (5) an atmospheric region above the dropshaft represented as a cylinder with a diameter of 1 m and a height of 6 m. In this study, the numerical model is discretized using boundary-fitted cells. The discretization process employs a cell size of 0.01 m, which is smaller than the size recommended by Chegini and Leon (2020), in order to effectively and accurately model the geyser through convergence analysis. Five boundary patches were prescribed for the numerical model: inlet, outlet, tank, pipe wall, and atmosphere. For inlet and outlet pressure data were prescribed. The *inlet* was applied with *prghTotalPressure* and *outlet* with *prghPressure*. The velocity (U) BCs for inlet and outlet are pressureInletOutletVelocity and inletOutlet, respectively. The atmospheric domain was kept as pressureInletOutletVelocity velocity and pressure as totalPressure; so that air could be exchanged if necessary. The boundary conditions for the tank were kept as pressureInletOutletVelocity velocity and totalPressure pressure. All the wall BC's were kept in a no-slip condition (i.e., velocity = 0). All walls are specified as wallFunctions, reducing the necessity of fined layered boundary layers and hence the computational time. For the automatic time step adjustment, adjustableRunTime was used with minimum $\Delta t = 10^{-8}$, keeping the maximum Courant-Friedrichs-Lewy/Courant $(CFL=u\Delta t/\Delta x)$ to 0.5. To ensure the stability of the model and improve its accuracy, the maximum value of the Courant number should be less than 1 (Courant et al., 1967).

This paper focuses on a singular case to elucidate the numerical study results, wherein the ratio between the initial water level in the dropshaft (h_w) and the dropshaft height (h_d) was established at 0.23. The primary mechanism, as encapsulated through numerical simulations, that induces geysering in the partially filled dropshaft system can be succinctly outlined as follows:

1. At t=12.3 s, the initial air pocket reaches the bottom of the dropshaft. This large air pocket enters the dropshaft and rises in the form of a Taylor-like bubble due to buoyancy. When the air penetrates the dropshaft, the hydrostatic head of the dropshaft decreases till it reaches 110,262 N/m² at t=13.58 s (Figure 5b). This sudden drop in hydrostatic pressure in the dropshaft creates a significant pressure gradient along the horizontal pipe. Figure 6(a) shows the variation of differential pressures (ΔP) measured during time interval t=11.5 s to 14 s. The ΔP_{16_25} represents the pressure difference between pressure at points P1 and P6. As speculated, no significant variations in differential pressures were observed till t=12.3 s due to the smooth advancement of air towards the dropshaft. As the

air enters the dropshaft, it builds the differential pressure along the horizontal pipe, causing an increase in pressure gradient and hence accelerating the air and water in the horizontal pipe.

Taitel and Dukler (1976) suggested KH instability to occur when the low pressure at the crest overcomes the stabilizing effect of gravity. The condition for wave growth is as shown in Equation (1);

$$U_G > \left[1 - \frac{h_L}{D}\right] \left[\frac{g(\rho_L - \rho_G)h_G}{\rho_G}\right]^{1/2} \tag{1}$$

where D is diameter of the horizontal pipe, U_G is the gas (i.e., air) velocity, h_L is liquid (i.e., water) height under stratified conditions, g is the gravitational acceleration, and ρ_G and ρ_L are the air and water densities, respectively. As shown in the Figure 6(b), the velocity of gas (U_G) in the horizontal pipe starts increasing as air start ingesting into the dropshaft, and at t=13.05 s, it overcomes the R.H.S. term of Equation (1). This satisfies the instability criteria to cause the transition from stratified to slug flow. It is worth mentioning that the KH instability provides a mechanism for initiating jumps and transitions; however, after the initial rise and fallback of water, the validity of instability criteria in the subsequent cycles is not guaranteed.

- 2. When the first slug passed the intersection, some liquid was siphoned into the dropshaft due to lower pressure, causing partial or complete blockage to the supply of air from the horizontal pipe. This stage is referred to as 'the blockage of dropshaft base.' As a consequence the pressure at the bottom of the dropshaft increases, pushing the air-water interface in the horizontal pipe further away from the dropshaft base and compressing the accumulated gas in the horizontal pipe. On the way up, air rises further into the dropshaft followed by a trailing mixture of air and water (like a churning flow), called slug jump. The ascending air inside the dropshaft causes the liquid film to rise to a certain height. However, the shear force acting on the film is not enough to balance the gravitational force due to the scarcity of air supply from the horizontal pipe. As a result, the film decelerated its upward velocity slowly and then accelerated to fall toward the junction. The flowing water through the horizontal pipe further carries falling film towards the downstream end. It should be noted that the ascending air could not produce the initial spillage due to the quite low initial water level in the dropshaft. The pressure at the dropshaft base decreases during this fallback stage (Figure 5b at t=14.4 s to 17.2 s).
- 3. The depressurization at the end of cycle 1 at t=17.2 s again causes a significant pressure gradient along the horizontal pipe, accelerating the air and water in the horizontal pipe. This relative rise in air and water velocity causes the formation of new slugs. When the slug reaches the intersection (at the base of the dropshaft), the water carryover into the dropshaft due to the slug flow repeat itself as described in cycle 1.
- 4. The sequence of rise and fall of the pressure gradient in Cycle 3 is similar to that described in cycle 1 and cycle 2. At this stage, the significantly less dense mixture started forming inside the dropshaft due to the continuous mixing of air due to the aforesaid cycles. At t=35.15 s air-water mixture rises to the top of the dropshaft, losing water, which quickly reduces the hydrostatic pressure. The depressurization due to spillage is significantly large, accelerating the air entering the dropshaft forming slugs inside the horizontal pipe. Once again the aforementioned liquid slugs cross the junction, creating

partial blockage at the intersection. It should be noted that the number of initial cycles required to create initial spillage (rise of the air-water mixture to the top of the dropshaft) is dependent on the initial water level in the dropshaft and the amount of air trapped into the horizontal pipe. The discussion in this study is only limited to the first eruption; however, the study showed that subsequent eruptions are observed in the system as long as a continuous supply of water and air is provided.

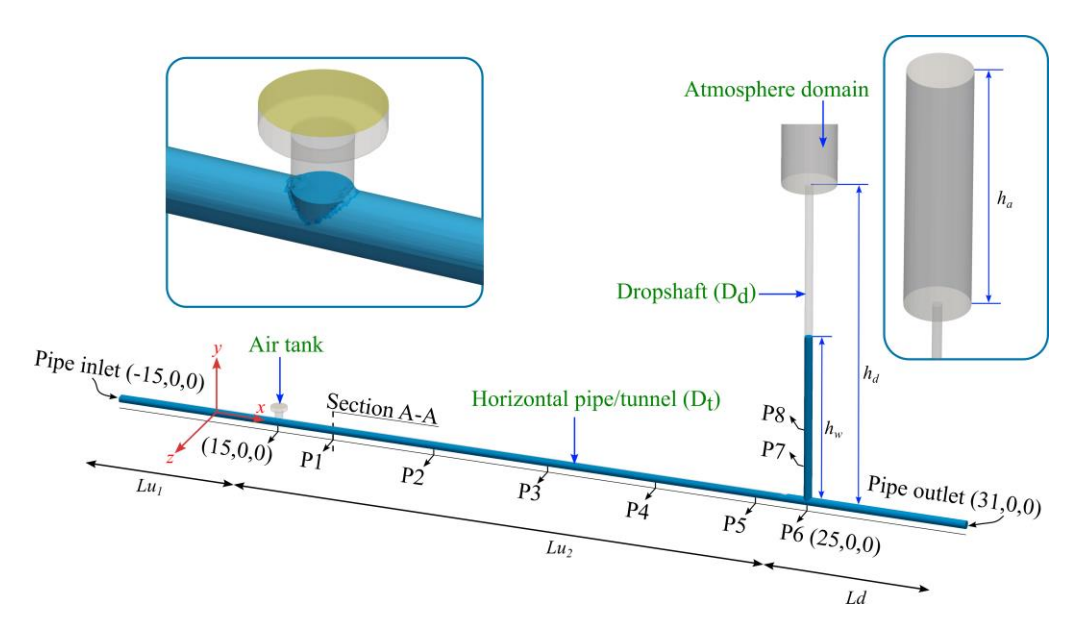


Figure 4. Schematic of the geyser computational setup and boundary conditions of the numerical model

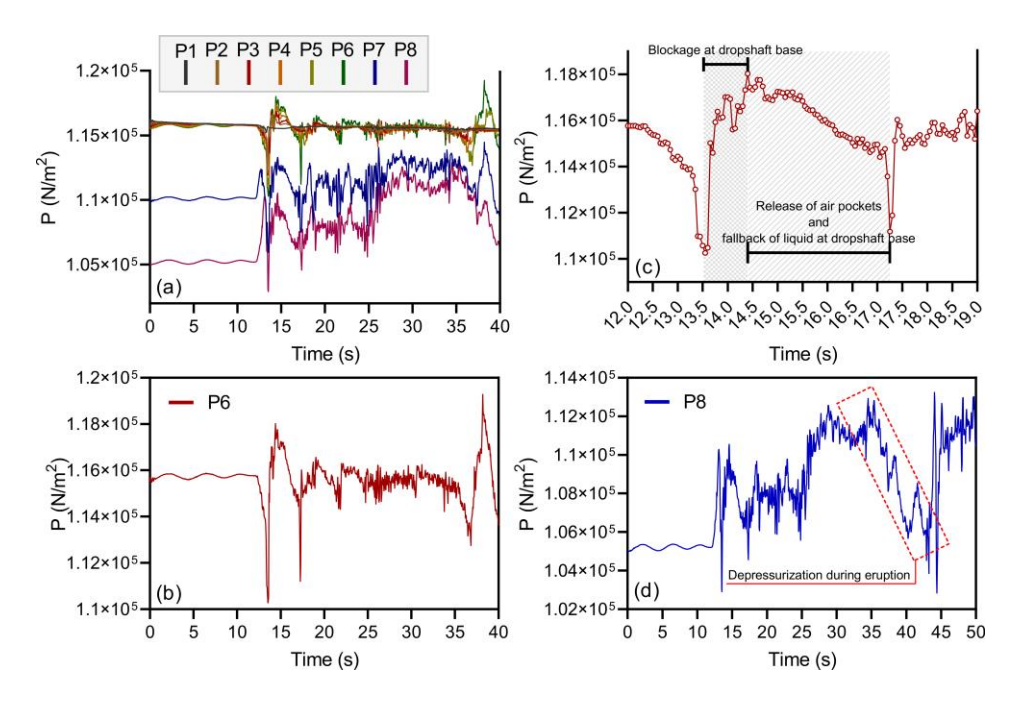


Figure 5. Results of simulation: (a) pressure recorded for all data points, (b) P6, (c) zoom-in P6, and (d) P8

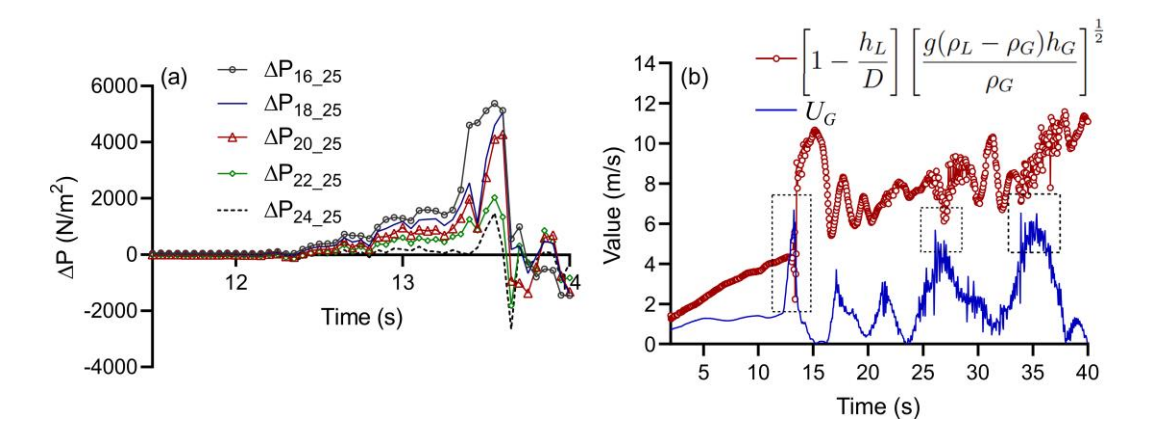


Figure 6. Results of simulation: (a) differential pressure along the horizontal pipe, (b) plot of instability criteria using Equation (1)

POTENTIAL RETROFITTING STRATEGIES TO ALLEVIATE THE STORMSEWER GEYSERS

This study briefly presents two potential near-surface retrofitting strategies, as follows:

- 1. Retrofitting Strategy I (chamber): Enlarging the diameter of a specific (near-surface) section of the dropshaft.
- 2. Retrofitting Strategy II (bypass): Adding a bypass combined with an adjacent orifice plate.

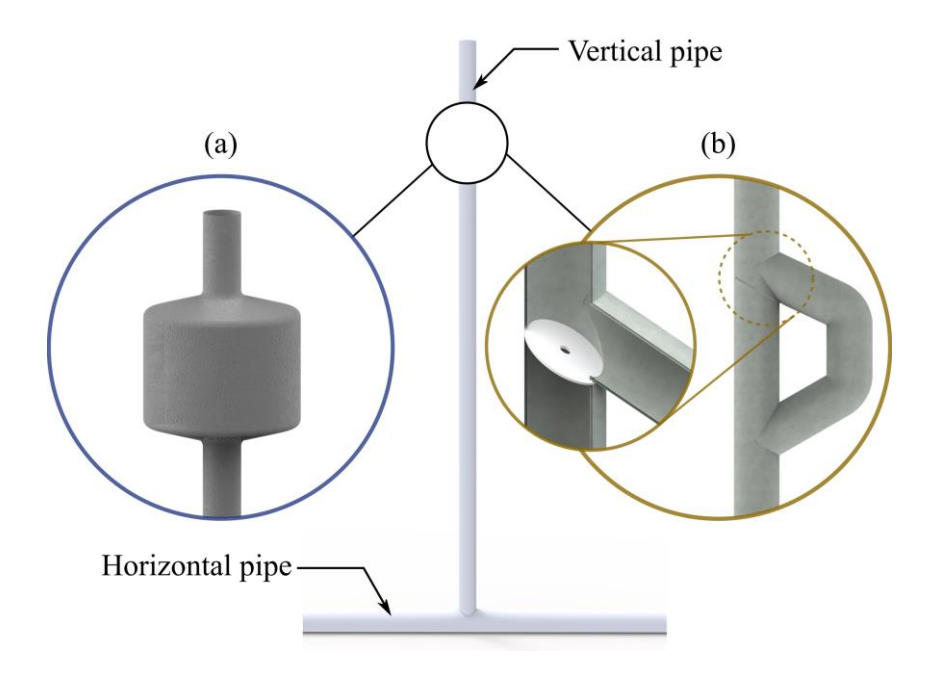


Figure 7. Results of simulation: (a) differential pressure along the horizontal pipe, (b) plot of instability criteria using Equation (1)

Through experimental and numerical investigations, the research demonstrated that the initial water spill induces depressurization, potentially resulting in the formation of slug flow within the

horizontal pipe and subsequent violent geyser eruptions. Furthermore, earlier studies indicated that a reduced dropshaft diameter contributes to increased eruption strength (Cong et al., 2017). With this understanding, the retrofitting strategy I was tailored to include an enlarged section of the dropshaft (also referred to as a chamber) with a diameter greater than that of the tunnel/horizontal pipe. Strategy II is inspired by earlier studies by Leon et al. (2019), which found that installing an orifice plate can effectively decrease the geyser height due to reduced air mass flow rate. However, installing only an orifice plate midway in the can have certain drawbacks, including a reduced cross-section that can impede the ability of the flow to enter the dropshaft freely and an increase in the amount of air transported downstream, potentially leading to geysering in other locations. Strategy II is a modified version in which an orifice plate is added to the dropshaft to take advantage of the benefits of an orifice plate for mitigating geysers while reducing its disadvantages by using a bypass.

This study briefly described the efficacy of the proposed retrofitting strategies by conducting a comparative analysis with the no-retrofitting scenario, employing a three-dimensional (3D) transient computational fluid dynamics model. The presented results are confined to a single case, reflecting limitations inherent in this paper. Specifically, the analysis focuses on a scenario with an initial water level in the dropshaft to the dropshaft height ratio of 0.5. Figure 8(a) shows the pressure variation at the bottom of the dropshaft for strategy I, II, and non-retrofitting case. When comparing the outcomes to the no-retrofitting case, it is evident that the bypass approach (strategy II) produces a lower pressure variation. On the other hand, for strategy I, the pressure variation was comparable to the no-retrofitting case, but there was a delay in reaching the maximum pressure drop. The ejection velocity in bypass strategy attains a value of 9.15 m/s at t=23.2 s (Figure 8(b)). Conversely, in the chamber strategy, the ejection velocity was almost identical to that in case without retrofitting. Although the use of an expansion chamber method reduced the initial rise of the water channel inside the dropshaft, a geyser event was still observed from the top of the dropshaft. The effectiveness of the chamber strategy can be improved by adding a deflector inside the chamber. Once the air-water mixture erupts inside the chamber, the mixture gets deflected by the deflector (i.e., helps separate the air from the water phase) instead of directly shooting upward; therefore, no visible air-water mixture can be observed. This holds true across various near-surface retrofitting strategies, where introducing an offset between the lower and upper sections of the dropshaft proves more effective in reducing visible geysers.

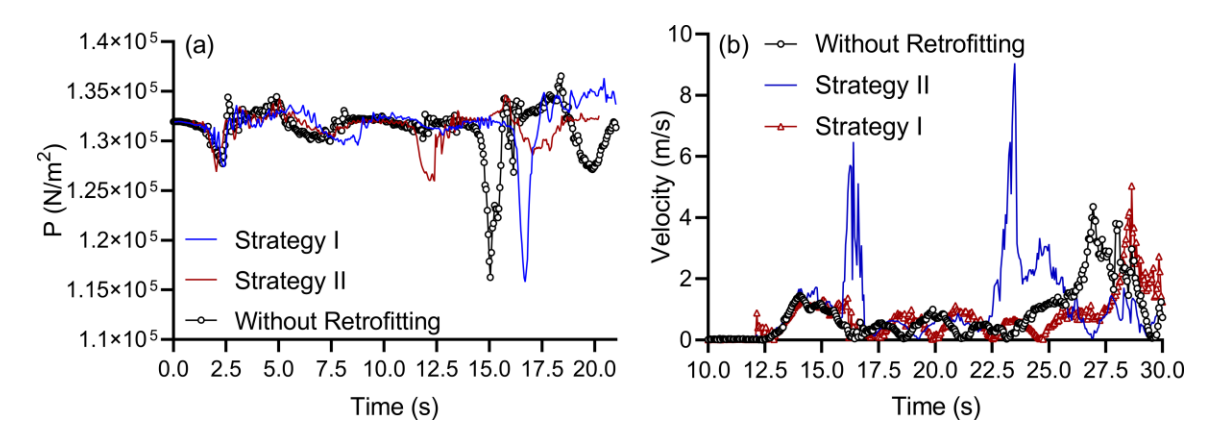


Figure 8. Quantitative results: (a) pressure variations for strategy I and II, (b) velocity variation at the exit of the dropshaft

CONCLUSION

This paper reports a field-scale laboratory and numerical study on sewer geysers in stormsewer systems and also assesses potential near-surface retrofitting strategies. The subsequent outcomes can be summarized as follows:

- (1) The geometric configuration used in field experiments promotes smooth air progression toward the dropshaft, fostering uniform air pocket development over the water surface in the horizontal pipe. This innovative approach enables a detailed exploration of flow transition mechanisms in the horizontal pipe and their correlation with the discharged airwater mixture from the vertical pipe.
- (2) A partially-filled dropshaft did not ensure immediate spillage at its top. The violent eruption is evident by the drastic reduction in the pressure head, creating a significantly large pressure gradient along the horizontal pipe resulting in flow transition.
- (3) The efficacy of near-surface strategies can be enhanced by introducing an offset between the lower and upper sections of the dropshaft. This offset effectively prevents the direct projection of the air and water mixture, consequently mitigating visible eruptions. It is crucial to conduct field monitoring to improve our understanding of the proposed retrofitting strategies.

ACKNOWLEDGMENT

The author gratefully acknowledges the financial support of the National Science Foundation (NSF) under Grant number 1928850. The views expressed are solely those of the authors. NSF does not endorse any products or commercial services mentioned.

REFERENCES

- Chegini, T., and Leon, A. S. (2020). "Numerical investigation of field-scale geysers in a vertical shaft." *Journal of Hydraulic Research*, 58(3), 503–515.
- Cong, J., Chan, S. N., and Lee, J. H. (2017). "Geyser formation by release of entrapped air from horizontal pipe into vertical shaft." *Journal of Hydraulic Engineering*, 143(9), 04017039.
- Courant, R., Friedrichs, K., and Lewy, H. (1967). "On the partial difference equations of mathematical physics." *IBM journal of Research and Development*, 11(2), 215–234.
- Leon, A. S., Elayeb, I. S., and Tang, Y. (2019). "An experimental study on violent geysers in vertical pipes." *Journal of hydraulic research*, 57(3), 283–294.
- Leon, A. S., and Zanje, S. R. (2019). "Experiments and Numerical Modeling of Field-scale geysers in Stormsewer Systems." *38th IAHR World Congress*, September 2019.
- Taitel, Y., and Dukler, A. E. (1976). "A model for predicting flow regime transitions in horizontal and near horizontal gas-liquid flow." *AIChE journal*, 22(1), 47–55.
- Vasconcelos, J. G., and Wright, S. J. (2005). "Experimental investigation of surges in a stormwater storage tunnel." *Journal of hydraulic Engineering*, 131(10), 853–861.
- Zanje, S. R., Bian, L., Verma, V., Yin, Z., and Leon, A. S. (2022a). "Siphon Break Phenomena Associated with Pipe Leakage Location." *Journal of Fluids Engineering*, 144(11), 111202.

- Zanje, S. R., Mahyawansi, P., Leon, A. S., and Lin, C.-X. (2022b). "CFD Modeling of Storm Sewer Geysers in Partially Filled Dropshafts." *World Environmental and Water Resources Congress* 2022, ASCE, 1187–1195 (June).
- Zhou, F., Hicks, F. E., and Steffler, P. M. (2002). "Observations of air-water interaction in a rapidly filling horizontal pipe." *Journal of hydraulic engineering*, 128(6), 635–639.